AD-A251 672

DEPARTMENT OF DEFENCE

DEFENCE SCIENCE AND TECHNOLOGY ORGANISATION

AERONAUTICAL RESEARCH LABORATORY

MELBOURNE, VICTORIA

DTIC
ELECTE
JUN 22 1992
S A D

Flight Mechanics Technical Memorandum 424

A RANKINE-HUGONIOT EMULATING (DENSITY vs. VELOCITY)
RELATIONSHIP FOR CFD USAGE WITHIN AN INVISCID SHOCK WAVE

by

B.W.B. SHAW

92-16347

Approved for public release

OCTOBER 1991

DEPARTMENT OF DEFENCE
DEFENCE SCIENCE AND TECHNOLOGY ORGANISATION
AERONAUTICAL RESEARCH LABORATORY

A RANKINE-HUGONIOT EMULATING (DENSITY vs. VELOCITY) RELATIONSHIP FOR CFD USAGE WITHIN AN INVISCID SHOCK WAVE

by

B.W.B. SHAW

SUMMARY

To enable the Full Potential Equation method of computing transonic inviscid flows to accurately predict the conditions at exit from a shock wave - a desirable aim which the method fails to achieve to a greater or lesser extent - an improved relationship has been derived between the density (p) and velocity (q) inside an inviscid shock wave. This relationship replaces the conventional isentropic, isenergic relationship normally applied there. The shock exit conditions thereby obtained are the correct Rankine-Hugoniot values, for all shock inlet Mach numbers.

Zonal application of this improved (p,q) shock wave internal relationship should eliminate the prime cause of solution inaccuracy when using the conservative Full Potential Equation method.

Two alternative versions of this relationship are provided; CFD usage will indicate which is superior.

The analysis has been applied first to normal shock waves and then extended to oblique shock waves.

DSTO ARL

MELBOURNE

POSTAL ADDRESS: Director, Aeronautical Research Laboratory
                    506 Lorimer Street, Fishermens Bend 3207
                    Victoria   Australia

Contents

i

List of Figures

1 INTRODUCTION

The abrupt changes occurring across a physical shock wave are not truly isentropic. Instead, they obey the Rankine-Hugoniot relationship and depart more and more from being isentropic flow changes as the shock wave strength increases, that is as the shock wave entry Mach number M_{in} increases. However the full potential equation (FPE) approach, which has been widely used (e.g. Refs. 1-8) in CFD solutions of the transonic flows past aerofoils, wings, bodies, wing-body combinations, intakes, cascades and helicopter blades, makes the approximation that changes of state are isentropic throughout the entire flow field including any shock wave(s) present. Thus when used with shocked flows the FPE flow model may well introduce significant errors (see Refs. 9, 10) in the computed physical quantities of the flow and thereby in the global quantities C_L, C_D etc. For air flowing through a normal shock wave these physical errors are listed in Table 1 and illustrated at Figs. 2-4. (In Table 1 ΔM_{ex} is the error in shock wave exit Mach number M_{ex}, ΔPR and ΔDR are the percentage errors in the pressure ratio PR and density ratio DR across the shock wave.)

These Table 1 errors vary approximately as a power of $(M_{in}^2 - 1)$, and as

M_{in}	ΔM_{ex}	$\Delta PR\%$	$\Delta DR\%$
1.0	0	0	0
1.1	$-.00_7$	1	$\frac{1}{2}$
1.3	$-.04_3$	$6\frac{1}{2}$	5
1.5	$-.09_1$	16	$13\frac{1}{2}$
1.6	$-.11_5$	$22\frac{1}{2}$	19

Table 1: ERRORS RESULTING FROM THE FPE APPROXIMATION OF A NORMAL SHOCK WAVE   ($\gamma = 1.4$)

M_{in} increases from 1.0 they are at first insignificant but in due course increase rapidly to large values. There is thus a need for an improved model of the flow changes across a shock wave, for use with the FPE approach, particularly for transonic flows with relatively high Mach numbers at the shock wave entry.

The mathematical formulation of the conservative FPE flow model consists of a set of equations in the FPE dependent variables — potential function Φ, velocity q (together with its components) and density ρ. In particular, it involves the use of an algebraic (ρ vs. q) equation that is based, as previously indicated, on the assumption of universally isentropic flow; this is the source of the errors mentioned above. The analysis which follows describes the development of an alternative (ρ vs. q) continuous relationship that is non-isentropic and that ensures that shock wave exit conditions are as given by the Rankine-Hugoniot relations. *The relationship applies only in the entire interior region of an "inviscid" shock wave wafer.* [1] It is intended for zonal use with FPE flow

---

[1] The phrase "shock wave wafer" is used here and subsequently to emphasize the small but

1

computations and should eliminate the errors referred to above. Elsewhere in the flow the usual FPE isentropic, isenergic flow law giving (ρ vs. q) would apply, though with an allowance downstream of the shock wave for the reduced stagnation density there.

In fashioning this relationship the principal aims have been that:

- The relationship should ensure the correct — i.e. Rankine-Hugoniot — values of velocity q and density ρ at exit from the shock wave wafer. Consequently mass, energy and total impulse must be conserved in the transition from entry to exit locations of the shock wave wafer.

- The flow quantities must be piecewise continuous across the shock wave wafer entry face.

It also appeared desirable that:

- ρ should be a monotonic function of q (to accord with physical reality), and

- The finally chosen algebraic expression for $\rho = \rho(q)$ should involve a minimum of computational effort, consistent with satisfying the first two requirements with high accuracy.

γ has been assumed to be 1.4.

2 CONDITIONS AT EXIT FROM A NORMAL SHOCK WAVE

The procedure adopted has been to derive first a (ρ,q) relationship for a normal shock wave. In the Appendix this has then been extended to the more general case of an oblique shock wave.

Using q, ρ, p and a to denote speed, density, pressure and speed of sound, the continuity, momentum and energy-conservation equations across a normal shock wave, with upstream and downstream conditions denoted by suffices "1" and "2" (Fig. 1 refers), are as follows:-

continuity

$$\rho_2 q_2 = \rho_1 q_1 \tag{1}$$

momentum

$$\rho_2 q_2^2 + p_2 = \rho_1 q_1^2 + p_1$$

i.e.

$$\rho_2 q_2^2 [1 + a_2^2/(\gamma q_2^2)] = \rho_1 q_1^2 [1 + a_1^2/(\gamma q_1^2)] \tag{2}$$

---

finite thickness of computational (as well as physical) shock waves.

$$'2' \qquad\qquad '1'$$

$$(q_2;\ \rho_2, p_2, a_2) \qquad\qquad (q_1;\ \rho_1, p_1, a_1)$$
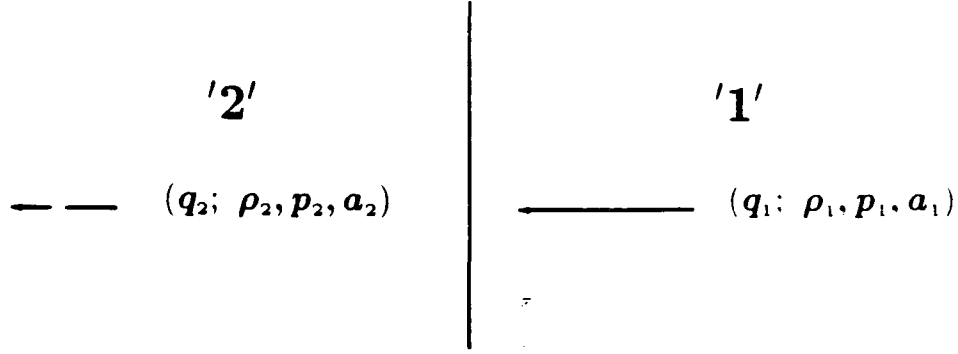
Figure 1: NORMAL SHOCKWAVE STATES

energy

$$q_2^2/2 + \frac{\gamma}{\gamma - 1} p_2/\rho_2 = q_1^2/2 + \frac{\gamma}{\gamma - 1} p_1/\rho_1$$

i.e.

$$\left.\begin{aligned}
\frac{\gamma - 1}{2} q_2^2 + a_2^2 &= \frac{\gamma - 1}{2} q_1^2 + a_1^2 \\
&= \frac{\gamma + 1}{2} q_\infty^{*2}
\end{aligned}\right\} \tag{3}$$

where $\{^{*}_{\infty}\}$ denotes sonic condition in the upstream flow, when achieved isentropically.

The set of four equations (1)-(3) yields the shock wave exit conditions, q_2, ρ_2, p_2 and a_2, in terms of the corresponding entry conditions and of q_∞^*. The solution is obtained as follows:

Dividing (2) by (1) and substituting for a_2^2 and a_1^2 from (3) yields

$$q_2 + q_\infty^{*2}/q_2 = q_1 + q_\infty^{*2}/q_1$$

or using (1) again

$$q_2 + (q_\infty^{*2}/\rho_1 q_1)\rho_2 = q_1 + q_\infty^{*2}/q_1 \tag{4}$$

Adopting $\hat{}$ to denote that the speeds and densities in (1) and (4) have been normalized by divisors q_∞^* and ρ_∞^*, and dropping the suffix "2", gives

$$\hat{\rho}\hat{q} = \hat{\rho}_1 \hat{q}_1 \tag{1'}$$

and

$$\hat{q} + \hat{\rho}/(\hat{\rho}_1 \hat{q}_1) = \hat{q}_1 + 1/\hat{q}_1 \tag{4'}$$

3

Thus for a given shock wave entry condition $(\hat{q}_1, \hat{\rho}_1)$, referring to Fig. 5 the shock wave exit condition $(\hat{q}_2, \hat{\rho}_2)$ is represented by the subsonic intersection B of rectangular hyperbola (1') (the continuity condition) with straight line (4') in the $(\hat{q}, \hat{\rho})$ plane, the other (supersonic) intersection being obviously the shock wave entry point A $(\hat{q}_1, \hat{\rho}_1)$ in Fig. 5.

Eliminating $\hat{\rho}$ from equations (1') and (4') yields a quadratic in $\hat{q}$:—

$$\hat{q}^2 - (\hat{q}_1 + 1/\hat{q}_1)\hat{q} + 1 = 0$$

with roots $\hat{q}_2$ and $\hat{q}_1$. Hence the product of the roots satisfies

$$\hat{q}_2 \hat{q}_1 = 1 \tag{5}$$

and combining this with (1) normalized gives

$$\hat{\rho}_2/\hat{\rho}_1 = \hat{q}_1^2 \tag{6}$$

With the aid of equations (5) and (6) it is possible to derive an analytical $\hat{\rho}$ vs. $\hat{q}$ relationship *at the exit* from a normal shock wave, i.e. to derive the locus of point "B" in Fig. 5 as the parameters $\hat{q}_1$ and $\hat{\rho}_1$ of the shock entry condition vary. This is achieved as follows:

At shock entry (suffix "1") the flow, which is isenergic throughout, has up to that point been also isentropic. So substituting $\hat{\rho}_1$ and $\hat{q}_1$ for $\hat{\rho}$ and $\hat{q}$ in the isentropic, isenergic channel flow equation

$$\hat{\rho} = \left(\frac{\gamma+1}{2} - \frac{\gamma-1}{2}\hat{q}^2\right)^{\frac{1}{(\gamma-1)}} \tag{7}$$

leads to

$$\hat{\rho}_1 = \left(\frac{\gamma+1}{2} - \frac{\gamma-1}{2}\hat{q}_1^2\right)^{\frac{1}{(\gamma-1)}} \tag{8}$$

With (6) this gives

$$\hat{\rho}_2 = \hat{q}_1^2 \left(\frac{\gamma+1}{2} - \frac{\gamma-1}{2}\hat{q}_1^2\right)^{\frac{1}{(\gamma-1)}}$$

and using (5)

$$\hat{\rho}_2 = \left\{\left(\frac{\gamma+1}{2} - \frac{\gamma-1}{2\hat{q}_2^2}\right)^{\frac{1}{(\gamma-1)}}\right\} / \hat{q}_2^2$$

i.e. dropping suffix "2"

$$\hat{\rho} = \left\{\left(\frac{\gamma+1}{2}\hat{q}^2 - \frac{\gamma-1}{2}\right)^{\frac{1}{(\gamma-1)}}\right\} / \hat{q}^{\frac{2\gamma}{(\gamma-1)}} \tag{9}$$

which simplifies to

$$\hat{\rho} = R \left(\frac{\gamma + 1}{2} - \frac{\gamma - 1}{2} R \right)^{\frac{1}{(\gamma - 1)}}$$

where $\qquad$ (9′)

$$R = 1/\hat{q}^2$$

The shock exit (density vs. speed) relationship (9) is presented on Fig. 5 as the $\hat{\rho}_{ex}$ vs. $\hat{q}$ curve, for $1 \geq \hat{q} \geq \sqrt{\frac{\gamma-1}{\gamma+1}} = \frac{1}{\sqrt{6}}$. As the normalized shock exit speed $\hat{q}$ decreases from 1.0, $\hat{\rho}_{ex}$ at first increases up to a maximum value of about 1.17: it then falls sharply to zero at $\hat{q} = \frac{1}{\sqrt{6}}$.

The maximum $\hat{\rho}_{ex}$ occurs when $\frac{d\hat{\rho}_{ex}}{d\hat{q}} = 0$ that is, differentiating (9′) logarithmically w.r.t. R, when

$$1/R - \left[0.5 / \left(\frac{\gamma + 1}{2} - \frac{\gamma - 1}{2} R \right) \right] = 0$$

giving the normalized exit speed

$$\hat{q} = 1/\sqrt{R} = \sqrt{\frac{\gamma}{\gamma + 1}} = .7638$$

(corresponding to a shock inlet Mach number of $\sqrt{2}$). Substituting this $\hat{q}$ value into (9) yields

$$(\hat{\rho}_{ex})_{MAX} = 1.166_{05}$$

Shown also on Fig. 5 is the isentropic, isenergic flow relationship (7) presented as the $\hat{\rho}_{is}$ vs. $\hat{q}$ curve, for the complete $\hat{q}$ range from $\sqrt{\frac{\gamma+1}{\gamma-1}}$ ($= \sqrt{6}$ and corresponds to infinite Mach number) down to 0. The subsonic intersection C of this curve with the continuity equation (1′) curve gives the shock exit conditions as predicted by the conventional FPE method. The wide gap between intersections B and C thus represents the difference between the Rankine-Hugoniot and FPE shock exit conditions. It demonstrates again, quite dramatically, the large and rapidly increasing error ($\hat{\rho}_C - \hat{\rho}_B$) in the shock exit density when determined by the conventional FPE method, particularly when B is to the left of peak "Π" of the $\hat{\rho}_{ex}$ curve (corresponding to the shock inlet Mach number exceeding $\sqrt{2}$).

So within a normal shock wave the following two-part (density~velocity) relationship will ensure Rankine-Hugoniot conditions at shock exit:—

$\hat{q} \geq 1 \qquad \hat{\rho} = \hat{\rho}_{is}(\hat{q}) \qquad - \qquad$ equation (7)

$\hat{q} \leq 1 \qquad \hat{\rho} = \hat{\rho}_{ex}(\hat{q}) \qquad - \qquad$ equation (9)

Adopting this approach, the only modification required to the FPE flow model *within* the shock wave is to use equation (9) instead of equation (7) for the subsonic ($\hat{q} \leq 1$) portion of the wave.

Note that equation (9) is conveniently parameter-free, i.e. it requires no knowledge of the shock wave inlet conditions $\hat{q}_1$ and $\hat{\rho}_1$ (unlike equation (4')).

Flow conditions downstream of the shock, consistent with the modified shock wave model, are dealt with later at §4.

The use of equation (9) has, however, two potential drawbacks, although these may be only slight or non-existent in many cases. Firstly the exit stagnation density, which is pivotal in determining the flow downstream of the shock wave, is affected by any error in the perceived shock exit location and state. Secondly, as indicated above and in Fig. 5, equation (9) when plotted has a slight peak — i.e. ceases to be monotonic — if $\hat{q} < .7638$; this happens only if $M_{in} > \sqrt{2}$. The peak, if it occurs, does so towards the shock wave exit and the density then declines until shock exit is reached. For $M_{in} < 1.6$ the decline is less than $2\frac{1}{3}\%$. Some local numerical instability might conceivably result from this peaking, during a CFD iterative solution of a transonic flow. However such instability could be prevented by clipping the density peak, so replacing it with a density plateau, and then progressively eliminating the clipping in suitably conrolled stages as the iterative solution proceeds.

To avoid these potential problems another (density~velocity) shock wave wafer relationship is developed in the following section.

3 SECOND PROPOSED DENSITY vs. VELOCITY RELATIONSHIP WITHIN THE SHOCK WAVE WAFER

Referring again to Fig. 5, virtually any more-or-less monotonic curve joining A to B (other than the continuity equation (1') curve) appears suitable as a replacement here for the isentropic, isenergic flow equation (7) of the FPE method. Such a curve would intersect the continuity equation (1') subsonically at B, which is on the ($\hat{\rho}_{ex}$ vs. $\hat{q}$) curve — thereby ensuring Rankine-Hugoniot exit conditions.

However, as previously mentioned, there exists a possible problem concerned with pinpointing computationally the precise location of X, the exit point of a streamline from the shock wave wafer (corresponding to state B in Fig. 5).[2] This is another changeover point for the (density vs. speed) relationship: proceeding streamwise along the streamline through X the ($\hat{\rho}$ vs. $\hat{q}$) relationship changes there from the shock wave wafer internal form

$$\hat{\rho}_{sw} = \hat{\rho}_{sw}(\hat{q}) \tag{10}$$

---

[2]One way of establishing computationally the location of X is to compute the spatial density gradient with respect to the streamwise, or nearly streamwise, coordinate of the flowfield. In the immediate vicinity of X this gradient is extremely large just upstream of X (being within the shock wave wafer) but very much smaller just downstream of X. Such a test thus enables X to be located approximately, with fair accuracy.

(not yet determined) to the isentropic.[3] isenergic form for flow downstream of X:—

$$\hat{\rho} = \hat{\rho}_B \left\{ \left(1 - \frac{\gamma - 1}{\gamma + 1}\hat{q}^2\right) \Big/ \left(1 - \frac{\gamma - 1}{\gamma + 1}\hat{q}_B^2\right) \right\}^{1/(\gamma-1)} \qquad (11)$$

Although this change is piece-wise continuous in ordinate, it is not necessarily so in gradient. If due to the computational discretization of the flow field. or for any other reason, a small normalized speed error $\Delta\hat{q}$ arises at X from a slightly inaccurate determination of the precise shock exit location X. then there will also be an error

$$\Delta\hat{q}\frac{d\hat{\rho}_{sw}}{d\hat{q}} \; =$$

in the value of $\hat{\rho}_B$ (as used in (11)). Consequently at the presumed (but slightly incorrect) shock exit state B there will be a fractional error — either overshoot or undershoot — in the normalized stagnation density

$$\left(\hat{\rho}_{sw} \Big/ \left[1 - \frac{\gamma - 1}{\gamma + 1}\hat{q}^2\right]^{1/(\gamma-1)}\right)_B$$

equal to

$$\Delta\hat{q}\left(\frac{d}{d\hat{q}}\log\left\{\hat{\rho}_{sw}\Big/\left[1 - \frac{\gamma - 1}{\gamma + 1}\hat{q}^2\right]^{1/(\gamma-1)}\right\}\right)_B$$
$$= \; \Delta\hat{q}\left(\frac{1}{\hat{\rho}_{sw}}\frac{d\hat{\rho}_{sw}}{d\hat{q}} + \frac{2\hat{q}}{\gamma + 1 - (\gamma - 1)\hat{q}^2}\right)_B \qquad (12)$$

correct to the first order in $\Delta\hat{q}$. As an accurate computation of the flowfield downstream of the shock wave depends on accurately determining the stagnation density at shock wave exit[4], it is important that the form of $\hat{\rho}_{sw}(\hat{q})$ should be chosen to make this error zero, if possible, but otherwise minimal.

Therefore from equation (12) a further desired condition, additional to those listed at §1, is

$$\left(\frac{1}{\hat{\rho}_{sw}}\frac{d\hat{\rho}_{sw}}{d\hat{q}}\right)_B = -\left(\frac{2\hat{q}}{\gamma + 1 - (\gamma - 1)\hat{q}^2}\right)_B \qquad (13)$$

Equation (13) in fact expresses the criterion that the stagnation density — as derived from (10) — is to be stationary just upstream of X. Downstream from X the stagnation density of the flow is constant along a given streamline (as expressed at equation (11)). Thus along a streamline, by imposing condition (13) there will be at X piece-wise continuity of the stagnation density not just in ordinate but also in first derivative w.r.t. $\hat{q}$.

This piece-wise continuity of stagnation density at X could be extended to any desired order of derivative w.r.t. $\hat{q}$ by suitable choice of the function $\hat{\rho}_{sw}(\hat{q})$ in (10). However it is best to restrict (10) to a second order polynomial in $\hat{q}$: third and higher order polynomials run the risk of possible non-physical intersections — i.e. intersections other than A and B in Fig. 5 — with equation (1′).

---

[3] *More precisely, isentropic along a streamline.*

[4] Refer to equation (11).

From (5) and (6) $B(\hat{q}_2, \hat{\rho}_2)$ is $(1/\hat{q}_1, \hat{\rho}_1\hat{q}_1{}^2)$; A is $(\hat{q}_1, \hat{\rho}_1)$. Also, substituting these B coordinates into (13), the desired slope $\frac{d\hat{\rho}_{\,\smile}}{d\hat{q}}$ at B of the proposed quadratic relationship (10) is

$$-2\hat{\rho}_1\hat{q}_1^3/[(\gamma + 1)\hat{q}_1^2 - (\gamma - 1)]$$

The desired $(\hat{\rho},\hat{q})$ equation (10) within the shock wave wafer is then readily verified as being

$$\hat{\rho}/\hat{\rho}_1 = (1 + \hat{q}_1^2) - \hat{q}_1\hat{q} - (\hat{q} - \hat{q}_1)(\hat{q} - 1/\hat{q}_1)\hat{q}_1^2/\left[\frac{\gamma + 1}{\gamma - 1}\hat{q}_1^2 - 1\right] \qquad (14)$$

Note that equation (14) really contains only one parameter. $\hat{q}_1$, because $\hat{\rho}_1$ is obtained immediately in terms of $\hat{q}_1$ from equation (8). Knowledge of $\hat{q}_1$ requires the determination of shock wave entry location; this is achieved in similar fashion to determining the shock wave exit X. (See footnote 2.)

An example of equation (14), for some chosen value of $\hat{q}_1$, is plotted in Fig. 6.

3.1 INTERSECTIONS OF EQUATION (14) WITH THE CONTINUITY EQUATION

Equation(14) intersects the continuity equation (1′) at just three points: for substituting (1′) into (14) yields a cubic in $\hat{q}$:—

$$\hat{q}_1 = (1 + \hat{q}_1^2)\hat{q} - \hat{q}_1\hat{q}^2 - \hat{q}(\hat{q} - \hat{q}_1)(\hat{q} - 1/\hat{q}_1)Q_1 \qquad (15)$$

where

$$Q_1 = \hat{q}_1^2/\left[\frac{\gamma + 1}{\gamma - 1}\hat{q}_1^2 - 1\right] \qquad (16)$$

Note here that since $\hat{q}_1 > 1$, therefore $Q_1 > \frac{\gamma - 1}{\gamma + 1} > 0$.

(15) is:—

$$-Q_1\hat{q}^3 + [Q_1(\hat{q}_1 + 1/\hat{q}_1) - \hat{q}_1]\hat{q}^2 + (\hat{q}_1^2 + 1 - Q_1)\hat{q} - \hat{q}_1 = 0$$

which factorizes to

$$(-Q_1\hat{q} - \hat{q}_1)(\hat{q} - \hat{q}_1)(\hat{q} - 1/\hat{q}_1) = 0$$

The roots of this are

$$\hat{q} = \hat{q}_1 \qquad \text{(point A),}$$
$$\hat{q} = 1/\hat{q}_1 \qquad \text{(point B)}$$
$$\text{and} \qquad \hat{q} = -\hat{q}_1/Q_1$$

Now $Q_1 > 0$. (Refer below (16).) Hence the third intersection $(\hat{q} = -\hat{q}_1/Q_1)$ is illusory because it corresponds to a negative value of $\hat{q}$. Thus there are only two possible intersections of (14) and (1′) — the two physical ones, A and B. as required. (See Fig. 6.)

8

3.2 MONOTONICITY OF EQUATION (14)

It is readily verified that equation (14) may be written as

$$\hat{\rho}/\hat{\rho}_1 = -Q_1\hat{q}^2 + [(Q_1 - 1)\hat{q}_1 + Q_1/\hat{q}_1]\hat{q} + [\hat{q}_1^2 + 1 - Q_1] \qquad (14')$$

Differentiating,

$$\frac{1}{\hat{\rho}_1}\frac{d\hat{\rho}}{d\hat{q}} = -2Q_1\hat{q} + [(Q_1 - 1)\hat{q}_1 + Q_1/\hat{q}_1]$$

and

$$\frac{d^2\hat{\rho}}{d\hat{q}^2} = -2Q_1\hat{\rho}_1 < 0$$

So $\hat{\rho}$ is stationary (a maximum in fact) only at

$$\begin{aligned}
\hat{q} = \bar{\bar{q}} &= [(1 - 1/Q_1)\hat{q}_1 + 1/\hat{q}_1]/2 = 1/\hat{q}_1 - [1/\hat{q}_1 - (1 - 1/Q_1)\hat{q}_1]/2 \\
&= 1/\hat{q}_1 - \hat{q}_1/\gamma - 1 \qquad \text{from (16)}
\end{aligned}$$

Thus, $\hat{q}_1$ being positive, $\bar{\bar{q}} < 1/\hat{q}_1$ (= $\hat{q}_2$, the $\hat{q}$ value at B). Hence in Fig. 6 the vertex of parabola (14') is to the left of B. Therefore over the range of application A to B parabolic arc (14') is monotonic and convex upward; within this range (as shown previously) it intersects the continuity equation (1') only at A and B.

4 CONDITIONS DOWNSTREAM OF THE SHOCK WAVE

In the FPE flow field model the flow is assumed to be universally isentropic; therefore the stagnation density and stagnation pressure are globally constant throughout the flow field. With the modified flow field model resulting from the new shock wave representation, however, these quantities — being dependent on the local shock inlet Mach number M_1 — now vary along the exit face of an embedded normal shock wave from its foot (M_1=body surface $M_1 > 1$) to its tip (M_1=1), and then remain constant downstream of the shock only along a given streamline.

4.1 DETERMINING THE STAGNATION DENSITY AT SHOCK WAVE EXIT

Stagnation density is defined by

$$\rho_{STAG} = \rho / \left[1 - \frac{\gamma - 1}{\gamma + 1}\hat{q}^2\right]^{1/(\gamma - 1)}$$

Therefore at shock wave exit the normalized stagnation density $\hat{\rho}_{STAG_B}$ is given by

$$\hat{\rho}_{STAG_B} = \rho_{STAG_B}/\rho_\infty^* = \hat{\rho}_B / \left[1 - \frac{\gamma - 1}{\gamma + 1}\hat{q}_B^2\right]^{1/(\gamma - 1)}$$

9

However exit state B lies on the B-locus ($\hat{\rho}$ vs. $\hat{q}$) curve defined by equation (9). So

$$\hat{\rho}_B = \left[\frac{\gamma-1}{2}\left(\frac{\gamma+1}{\gamma-1}\hat{q}_B^2 - 1\right)\Big/\hat{q}_B^{2\gamma}\right]^{1/(\gamma-1)}$$

Therefore substituting for $\hat{\rho}_B$,

$$\hat{\rho}_{STAG_B} = \left\{\left(\frac{\gamma-1}{2}\right)\frac{\left[\frac{\gamma+1}{\gamma-1}\hat{q}_B^2 - 1\right]}{\hat{q}_B^{2\gamma}\left[1 - \frac{\gamma-1}{\gamma+1}\hat{q}_B^2\right]}\right\}^{1/(\gamma-1)} \tag{17}$$

4.2 BODY SURFACE PRESSURES

The normalized stagnation pressure at shock wave exit, $\hat{p}_{STAG_B}$, is readily derived from the fact that the stagnation temperature, T_{STAG}, is constant throughout the isenergic flow. Thus:—

$$\frac{\hat{p}_{STAG_B}}{\hat{p}_{STAG_\infty}} = \frac{\hat{\rho}_{STAG_B}}{\hat{\rho}_{STAG_\infty}}\frac{T_{STAG_B}}{T_{STAG_\infty}} = \frac{\hat{\rho}_{STAG_B}}{\hat{\rho}_{STAG_\infty}} \tag{18}$$

(where pressures are normalized by the divisor p_∞^*).

Now

$$\hat{\rho}_{STAG_\infty} = \rho_{STAG_\infty}/\rho_\infty^* = \text{critical density ratio} = \left(\frac{\gamma+1}{2}\right)^{1/(\gamma-1)}$$

and

$$\hat{p}_{STAG_\infty} = p_{STAG_\infty}/p_\infty^* = \text{critical presssure ratio} = \left(\frac{\gamma+1}{2}\right)^{\gamma/(\gamma-1)}$$

Therefore inserting these values into (18)

$$\hat{p}_{STAG_B} = \left(\frac{\gamma+1}{2}\right)\hat{\rho}_{STAG_B}$$

with $\hat{\rho}_{STAG_B}$ determined from (17). Along the body surface streamline $\hat{p}_{STAG}$ is (discontinuously) constant, with the values $\hat{p}_{STAG_\infty}$ upstream and $\hat{p}_{STAG_B}$ downstream, respectively, of the shock wave. Also $\hat{q}$ is known throughout the flowfield, and in particular on the body surface, from the converged flow solution. Hence the body surface pressure distribution is immediately calculable from

$$\hat{p} = \hat{p}_{STAG}\left[1 - \frac{\gamma-1}{\gamma+1}\hat{q}^2\right]^{\gamma/(\gamma-1)}$$

5 CONCLUDING REMARKS

1. In view of the importance of correctly predicting shock wave exit conditions in CFD solutions of shocked transonic flows, a new improved relationship has

been derived between density (ρ) and velocity (q) *inside* an inviscid normal shock wave. This relationship is much superior to that conventionally applied there by the conservative full potential equation (FPE) method and should improve very considerably its accuracy and range of applicability, especially for flows containing strong shock waves.

2. In deriving the improved (ρ,q) relationship the FPE assumption of globally isentropic flow has been discarded inside the normal shock wave and, instead, the correct physical conditions at shock exit have been enforced. Additionally, the relationship (equation (14)) ensures that the shock exit stagnation density, a vital element in determining the post-shock flow, is unaffected (to the first order) by any small error that may be present in the perceived shock wave exit location (and state).

3. The only parameter appearing in the new (ρ,q) relationship (14) is the normalized velocity (or alternatively the Mach number) at shock entry. This can be determined — and continuously updated — from the developing iterative flow field solution once the shock becomes recognisable.

4. An alternative version of the (ρ,q) relationship, equation (9), which has the advantage of being parameter-free, is also presented. With this relationship, however, the exit stagnation density is subject to any error in the perceived shock wave exit location (and state). As well, if the normal shock wave inlet Mach number M_1 is higher than $\sqrt{2}$ a slight non-monotonicity develops in this alternative (ρ,q) relationship. This occurs near to the shock wave exit, with the density peaking and then declining slightly to its value at exit. The density decline is at most only $2\frac{1}{2}\%$ for $M_1 \leq 1.6$. In theory this peaking effect might conceivably trigger some numerical instability in an iterative computational solution. Such instability can be avoided by clipping the density peak, thus replacing it with a density plateau, and then progressively eliminating the clipping in suitably controlled stages as the iterative solution proceeds.

5. The two versions of the improved (ρ,q) relationship applicable inside an inviscid normal shock wave are given by equations (14) and (9) (as stated); CFD usage will indicate which is superior.

6. A simple rule for extending the (ρ.q) relationship to the case of an oblique shock wave is given in the Appendix; equations (A22), (A22ob), (A25) and (A26) refer.

REFERENCES

1. Holst, T.L. and Thomas, S.D. Numerical Solution of Transonic Wing Flow Fields. AIAA-82-0105, 1982.

2. Dougherty, F.C., Holst, T.L., Gundy, K.L. and Thomas, S.D. TAIR — A Transonic Airfoil Analysis Computer Code. NASA TM-81296, 1981.

3. South, J.C. and Jameson, A. Relaxation Solutions for Inviscid Axisymmetric Transonic Flow Over Blunt or Pointed Bpdies. ARC 34-726, 1973.

4. Raj, P. and Reaser, J.S. An Improved Full-Potential Finite-Difference transonic-Flow Code (FLO-22.5) for Wing Analysis and Design. Lockheed-California LR 29759, 1981.

5. Caughy, D.A. and jameson, A. Progress in Finite-Volume Calculations for Wing Fuselage Combinations. AIAA J, 18, 11, Nov. 1980.

6. Chen, L.T. and Caughey, D.A. High-Order Finite Difference Scheme for Three-Dimensional transonic Flowfields About Axisymmetric Bodies. J. Aircraft, 17, 9, Sep. 1980.

7. Kwak, D. Am Implicit Transonic Full Potential Code for Cascade Flow on H-Grid Topology. AIAA 83-0506, 1983.

8. Costes, M. and Jones, H.E. Computation of Transonic Potential Flow on Helicopter Rotor Blades. ONERA-1987-138, 1987.

9. Steinhoff, J. and Jameson, A. Multiple Solutions of the Transonic Potential Flow Equation. AIAA 81-1019, 1981.

10. Salas, M.D. and Gumbert, C.R. Breakdown of the Conservative Potential Equation. NASA Tech. Paper 2359, 1986.

11. Murduchow, M. and Libby, P.A. On the Complete Solution of the One-Dimensional Flow Equations of a Viscous Heat-Conducting Compressible Gas. J. Aero. Sci. 16, 11, 1949.

12. Von Neumann, J. and Richtmeyer, R.D. A Method for the Numerical Calculation of Hydrodynamic Shocks. J. App. Phys, 21, 3, 1950.

13. Liepmann, H.W., Narisima, R. and Chahine, M.T. Structure of a Plane Shock Layer. Phys. Fluids, 5, 11, 1962.

14. Talbot, L. and Scale, S.M. Shock Wave Structure in a Relaxing Diatomic Gas. Rarified Gas Dynamics — Proc. 2nd Int. Symp. on Rarified Gas Dynamics at Univ. of Calif. Academic Press, New York, 1961.

15. Pike, J. Notes on the Structure of Viscous and Numerically-Captured Shocks. Aero. J., 89, 889, 1985.

Appendix A

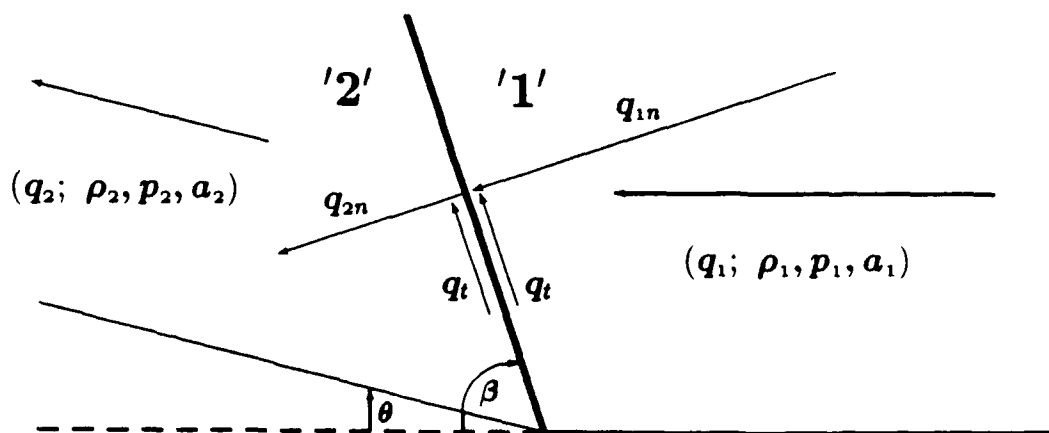# EXTENSION TO OBLIQUE SHOCK WAVES

Figure A1: OBLIQUE SHOCKWAVE STATES

A1   FUNDAMENTAL AND DERIVED EQUATIONS

When the shock wave is oblique, the continuity, momentum and energy equations become with the notation of Fig. A1:—

continuity

$$\rho_2 q_{2n} = \rho_1 q_{1n} = \text{mflux} \qquad (A1)$$

(where mflux is the mass flux rate normal to the shock wave and (q_{1n}, q_t), (q_{2n}, q_t) are the velocity components normal and parallel to the shockwave at entry and exit)

momentum

$$(p_2 - p_1) = \text{mflux}(q_{1n} - q_{2n}) \qquad (A2)$$

13

which, using equation (A1), may be written as

$$q_{1n}^2 - q_{2n}^2 = \frac{(q_{1n} + q_{2n})(p_2 - p_1)}{\text{mflux}} = \left(\frac{1}{\rho_1} + \frac{1}{\rho_2}\right)(p_2 - p_1) \qquad (A3)$$

energy (@ '1')

$$\left(\frac{q_{1n}^2}{2} + \frac{q_t^2}{2}\right) + \frac{\gamma}{\gamma - 1}\frac{p_1}{\rho_1} = \frac{\gamma + 1}{2(\gamma - 1)}q_\infty^{*2} \qquad (A4)$$

energy (@ '2')

$$\left(\frac{q_{2n}^2}{2} + \frac{q_t^2}{2}\right) + \frac{\gamma}{\gamma - 1}\frac{p_2}{\rho_2} = \frac{\gamma + 1}{2(\gamma - 1)}q_\infty^{*2} \qquad (A5)$$

Expressions for q_{2n} and ρ_2 analagous to those for the normal shock wave case are found as follows.

Differencing equations (A4) and (A5) gives

$$q_{1n}^2 - q_{2n}^2 = \frac{2\gamma}{\gamma - 1}\left(\frac{p_2}{\rho_2} - \frac{p_1}{\rho_1}\right) \qquad (A6)$$

Combining equations (A3) and (A6)

$$\left(\frac{1}{\rho_1} + \frac{1}{\rho_2}\right)(p_2 - p_1) = \frac{2\gamma}{\gamma - 1}\left(\frac{p_2}{\rho_2} - \frac{p_1}{\rho_1}\right)$$

i.e.

$$\left(\frac{\rho_2}{\rho_1} + 1\right)\left(\frac{p_2}{p_1} - 1\right) = \frac{2\gamma}{\gamma - 1}\left(\frac{p_2}{p_1} - \frac{\rho_2}{\rho_1}\right)$$

which leads to

$$\frac{p_2}{p_1} = \frac{\left(\frac{\gamma + 1}{\gamma - 1}\right)\frac{\rho_2}{\rho_1} - 1}{\left(\frac{\gamma + 1}{\gamma - 1}\right) - \frac{\rho_2}{\rho_1}} \qquad (A7)$$

ρ_2/ρ_1 may be found in terms of the initial state '1' as follows:-

From equations (A2) and (A1)

$$q_{1n} - q_{2n} = \frac{p_2}{\rho_2 q_{2n}} - \frac{p_1}{\rho_1 q_{1n}}$$

$$= \left(\frac{\gamma - 1}{\gamma}\right)\left\{\frac{\left[\frac{\gamma + 1}{2(\gamma - 1)}q_\infty^{*2} - \frac{q_t^2}{2}\right]}{q_{2n}} - \frac{q_{2n}}{2} - \frac{\left[\frac{\gamma + 1}{2(\gamma - 1)}q_\infty^{*2} - \frac{q_t^2}{2}\right]}{q_{1n}} + \frac{q_{1n}}{2}\right\}$$

from equations (A5) and (A4). Hence

$$(q_{1n} - q_{2n}) = \frac{(q_{1n} - q_{2n})}{2}\left\{\frac{\left[(\frac{\gamma + 1}{\gamma})q_\infty^{*2} - (\frac{\gamma - 1}{\gamma})q_t^2\right]}{q_{2n}q_{1n}} + \frac{\gamma - 1}{\gamma}\right\}$$

Since $q_{2n} \neq q_{1n}$, therefore

$$2 = \frac{(\frac{\gamma + 1}{\gamma})q_\infty^{*2} - (\frac{\gamma - 1}{\gamma})q_t^2}{q_{2n}q_{1n}} + \frac{\gamma - 1}{\gamma}$$

14

giving

$$q_{2n}q_{1n} = q_{\infty}^{*2} - (\tfrac{\gamma-1}{\gamma+1})q_t^2 \qquad (A8)$$

From (A1) and (A8)

$$\frac{\rho_2}{\rho_1} = \frac{q_{1n}}{q_{2n}} = \frac{q_{1n}^2}{q_{\infty}^{*2} - (\tfrac{\gamma-1}{\gamma+1})q_t^2} \qquad (A9)$$

So with equations (A8) and (A9) — together with energy equations (A4) and (A5) - in mind. replace q_{∞}^* as a normalizer by $\bar{q}^* = \sqrt{q_{\infty}^{*2} - (\tfrac{\gamma-1}{\gamma+1})q_t^2}$. Equation (A8) then becomes

$$\left(\frac{q_{2n}}{\bar{q}^*}\right)\left(\frac{q_{1n}}{\bar{q}^*}\right) = 1 \qquad (A10)$$

which is analogous to equation (5) of the main text for a normal shock wave. Now referring to Fig. A1,

$$\bar{q}^{*2} = \left[q_{\infty}^{*2} - (\tfrac{\gamma-1}{\gamma+1})q_t^2\right] = \left[q_{\infty}^{*2} - (\tfrac{\gamma-1}{\gamma+1})q_1^2\cos^2\beta\right] \qquad (A11)$$

β being the acute angle between the oblique shock wave and the velocity vector $\bar{q}_1$ at entry

$$= \left(\frac{\gamma-1}{\gamma+1}\right)q_1^2\left[\left(1 + \frac{2}{(\gamma-1)M_1^2}\right) - \cos^2\beta\right]$$

(from main text equation
(3) with $M_1 = q_1/a_1$)

$$= \left(\frac{\gamma-1}{\gamma+1}\right)q_1^2\left[\sin^2\beta + \frac{2}{(\gamma-1)M_1^2}\right] = q_{\infty}^{*2}\left[\frac{\sin^2\beta + \frac{2}{(\gamma-1)M_1^2}}{1 + \frac{2}{(\gamma-1)M_1^2}}\right]$$

(using (3) again).

i.e. since $q_1\sin\beta = q_{1n}$

$$\bar{q}^{*2} = \left(\frac{\gamma-1}{\gamma+1}\right)q_{1n}^2\left[1 + \frac{2}{(\gamma-1)M_1^2\sin^2\beta}\right] = q_{\infty}^{*2}\left[\frac{1 + (\tfrac{\gamma-1}{2})M_1^2\sin^2\beta}{1 + (\tfrac{\gamma-1}{2})M_1^2}\right] \qquad (A12)$$

A2   COMPARISON WITH NORMAL SHOCK WAVE RE-SULTS

Now from (A11) the energy equations (A4) and (A5) become:-

$$\frac{q_{1n}^2}{2} + \frac{\gamma}{\gamma-1}\frac{p_1}{\rho_1} = \frac{\gamma+1}{2(\gamma-1)}\bar{q}^{*2} \qquad (A4')$$

and

$$\frac{q_{2n}^2}{2} + \frac{\gamma}{\gamma-1}\frac{p_2}{\rho_2} = \frac{\gamma+1}{2(\gamma-1)}\bar{q}^{*2} \qquad (A5')$$

15

Also the continuity and momentum equations (previously presented in this Appendix) are:—

$$\rho_1 q_{1n} = \rho_2 q_{2n} = mflux \qquad (A1)$$

and

$$(p_2 - p_1) = mflux(q_{1n} - q_{2n}) \qquad (A2)$$

These four equations are formally identical to those for a normal shock wave provided that:—

Eqn. nos.	OBLIQUE S.W.	— Replacing —	NORMAL S.W.
(A1), (A2), (A4′)	q_{1n}	"	q_1
(A1), (A2), (A5′)	q_{2n}	"	q_2
(A12)	$\bar{q}^{*2} \left(= \dfrac{1+\left[\frac{\gamma-1}{2}\right]M_1^2 \sin^2\beta}{1+\left[\frac{\gamma-1}{2}\right]M_1^2} q_\infty^{*2} \right)$	"	q_∞^{*2}

From the above four basic equations (A4′), (A5′), (A1) and (A2) the following results can be derived (via the equations tabulated):—

(A10)	$q_{1n}q_{2n} = \bar{q}^{*2}$	"	$q_1 q_2 = q_\infty^{*2}$
(A9) with (A12)	$\dfrac{p_2}{p_1} = \dfrac{(\gamma+1)M_1^2 \sin^2\beta}{2+(\gamma-1)M_1^2 \sin^2\beta}$	"	$\dfrac{p_2}{p_1} = \dfrac{(\gamma+1)M_1^2}{2+(\gamma-1)M_1^2}$
DITTO with (A7)	$\dfrac{p_2}{p_1} = \dfrac{2\gamma}{\gamma+1}M_1^2 \sin^2\beta - \dfrac{\gamma-1}{\gamma+1}$	"	$\dfrac{p_2}{p_1} = \dfrac{2\gamma}{\gamma+1}M_1^2 - \dfrac{\gamma-1}{\gamma+1}$

Thus from the two tables above if $\left\{ \begin{array}{l} q_{1n} \text{ and } q_{2n} \text{ replace } q_1 \text{ and } q_2 \\ \bar{q}^* \text{ replaces } q_\infty^* \\ M_1 \sin\beta \text{ replaces } M_1 \end{array} \right\}$ (A13)

then the basic equations and the results derived therefrom are the same for an oblique shock wave as for a normal shock wave.

One further replacement is required, that for the density normalizer ρ_∞^*. This is obtained as follows:—

Considering the density at the shock wave entry face

$$\left(\frac{\rho_1}{\rho_\infty^*}\right)^{\gamma-1} = \left[1 - \frac{\gamma-1}{\gamma+1}\left(\frac{q_1}{q_\infty^*}\right)^2\right] / \left[1 - \frac{\gamma-1}{\gamma+1}\right] \qquad (A14)$$

(This is essentially the same equation as main text equation (8).) Therefore

$$2\left(\frac{\rho_1}{\rho_\infty^*}\right)^{\gamma-1} = \gamma + 1 - (\gamma-1)\left(\frac{q_1^2}{q_\infty^{*2}}\right) = \frac{1}{q_\infty^{*2}}\left[\gamma(q_\infty^{*2} - q_1^2) + q_\infty^{*2} + q_1^2\right] \qquad (A15)$$

Now $\qquad\qquad\qquad\qquad q_1^2 = q_{1n}^2 + q_t^2$

and from (A11) $\qquad\qquad q_\infty^{*2} = \bar{q}^{*2} + (\frac{\gamma-1}{\gamma+1})q_t^2$ $\qquad\qquad$ (A16)

16

Substituting from (A16) for q_1^2 and q_∞^{*2} into (A15) gives

$$2\left(\frac{\rho_1}{\rho_\infty^*}\right)^{\gamma-1} = \left[\gamma\left(\bar{q}^{*2} - q_{1n}^2 - \frac{2}{\gamma+1}q_{1t}^2\right) + \left(\bar{q}^{*2} + q_{1n}^2 + \frac{2\gamma}{\gamma+1}q_{1t}^2\right)\right]/q_\infty^{*2}$$

$$= \left[(\gamma+1)\bar{q}^{*2} - (\gamma-1)q_{1n}^2\right]/q_\infty^{*2}$$

Therefore

$$\frac{q_\infty^{*2}}{\bar{q}^{*2}}\left(\frac{\rho_1}{\rho_\infty^*}\right)^{\gamma-1} = \left[(\gamma+1) - (\gamma-1)q_{1n}^2/\bar{q}^{*2}\right]/2 = \left[\frac{1 - \frac{\gamma-1}{\gamma+1}\left(\frac{q_{1n}}{\bar{q}^*}\right)^2}{1 - \frac{\gamma-1}{\gamma+1}}\right] \qquad (A17)$$

Now let
$$(\bar{q}^{*2}/q_\infty^{*2})\,\rho_\infty^{*(\gamma-1)} = \bar{\rho}^{*(\gamma-1)}$$
i.e.
$$\left. \bar{\rho}^* = \rho_\infty^*(\bar{q}^*/q_\infty^*)^{2/(\gamma-1)} \right\} \qquad (A18)$$

Therefore from (A12)

$$\bar{\rho}^* = \rho_\infty^*\left\{\left[1 + \frac{\gamma-1}{2}M_1^2\sin^2\beta\right]/\left[1 + \frac{\gamma-1}{2}M_1^2\right]\right\}^{\frac{1}{(\gamma-1)}} \qquad (A19)$$

Substituting (A18) into (A17) leads to

$$\left(\frac{\rho_1}{\bar{\rho}^*}\right)^{\gamma-1} = \left[1 - \frac{\gamma-1}{\gamma+1}\left(\frac{q_{1n}}{\bar{q}^*}\right)^2\right]/\left[1 - \frac{\gamma-1}{\gamma+1}\right] \qquad (A20)$$

with $\bar{\rho}^*$ given by (A18).

(A20) is formally identical to main text equation (8) but with

$$\left\{\begin{array}{l} \bar{\rho}^* \text{ replacing } \rho_\infty^* \\ \bar{q}^* \text{ replacing } q_\infty^* \\ q_{1n} \text{ replacing } q_1 \end{array}\right\} \qquad (A21)$$

Thus for an oblique shock wave the appropriate density normalizer is $\bar{\rho}^*$.

A3 DENSITY vs. VELOCITY RELATIONSHIP FOR OBLIQUE SHOCKS

The (ρ vs. q) law that has been derived for the interior of a *normal* shock wave can be written as

$$\frac{\rho}{\rho_\infty^*} = \text{function}\left(\frac{q^2}{q_\infty^{*2}}\right) \qquad (A22)$$

This equation is adapted to the oblique shock wave case by applying appropriate replacements as indicated by (A13) and (A21), yielding

$$\frac{\rho}{\bar{\rho}^*} = \text{function}\left(\frac{q_n^2}{\bar{q}^{*2}}\right) = \text{function}\left(\frac{q^2}{\bar{q}^{*2}} - \frac{q_t^2}{\bar{q}^{*2}}\right) = \text{function}(k_2\bar{q}^2 - k_3)$$

i.e.

$$\tilde{\rho} = k_1 \text{function}(k_2\hat{q}^2 - k_3) \qquad (\text{A22ob})$$

with:

$$k_1 = \bar{\rho}^*/\rho_\infty^* = \left\{[1 + 0.2M_1^2\sin^2\beta]/[1 + 0.2M_1^2]\right\}^{2.5} \quad \text{by (A19)}$$

$$k_2 = q_\infty^{*2}/\bar{q}^{*2} = [1 + 0.2M_1^2]/[1 + 0.2M_1^2\sin^2\beta] \quad \text{by (A12)}$$

and

$$k_3 = q_t^2/\bar{q}^{*2} = (q_1^2\cos^2\beta/q^{*2})(q_\infty^{*2}/\bar{q}^{*2})$$

$$= \left[\frac{\frac{\gamma+1}{2}M_1^2\cos^2\beta}{1 + \frac{\gamma-1}{2}M_1^2}\right]\left[\frac{1 + \frac{\gamma-1}{2}M_1^2}{1 + \frac{\gamma-1}{2}M_1^2\sin^2\beta}\right]$$

by main text equation (3) and equation (A12);

hence

$$k_3 = 1.2M_1^2\cos^2\beta/[1 + 0.2M_1^2\sin^2\beta]$$

$$(\text{A23})$$

Using the isentropic isenergic flow relationship at equation (3) again, M_1^2 is given by

$$M_1^2 = 5(q_1^2/q_\infty^{*2})/(6 - q_1^2/q_\infty^{*2}) = 5\hat{q}_1^2/(6 - \hat{q}_1^2) \qquad (\text{A24})$$

leading to

$$k_2 = \frac{1}{1 - (\hat{q}_1^2\cos^2\beta)/6} \qquad (\text{A25})$$

From (A23) k_1, k_2 and k_3 are inter-related thus:

$$\left.\begin{array}{rcl} k_1 & = & k_2^{-2.5} \\ \text{and} \quad k_3 & = & 6(k_2 - 1) \end{array}\right\} \qquad (\text{A26})$$

Equation (A22) thus converts, by simple linear transformations, into the (more general) oblique shock wave case (A22ob), with the aid of equations (A25) and (A26).

Note that the angle β appearing in equation (A25) is a function of M_1 and θ, the flow deflection angle (see Fig. A1). Hence from (A25) and (A24) k_2 is a function of $\hat{q}_1$ and θ.
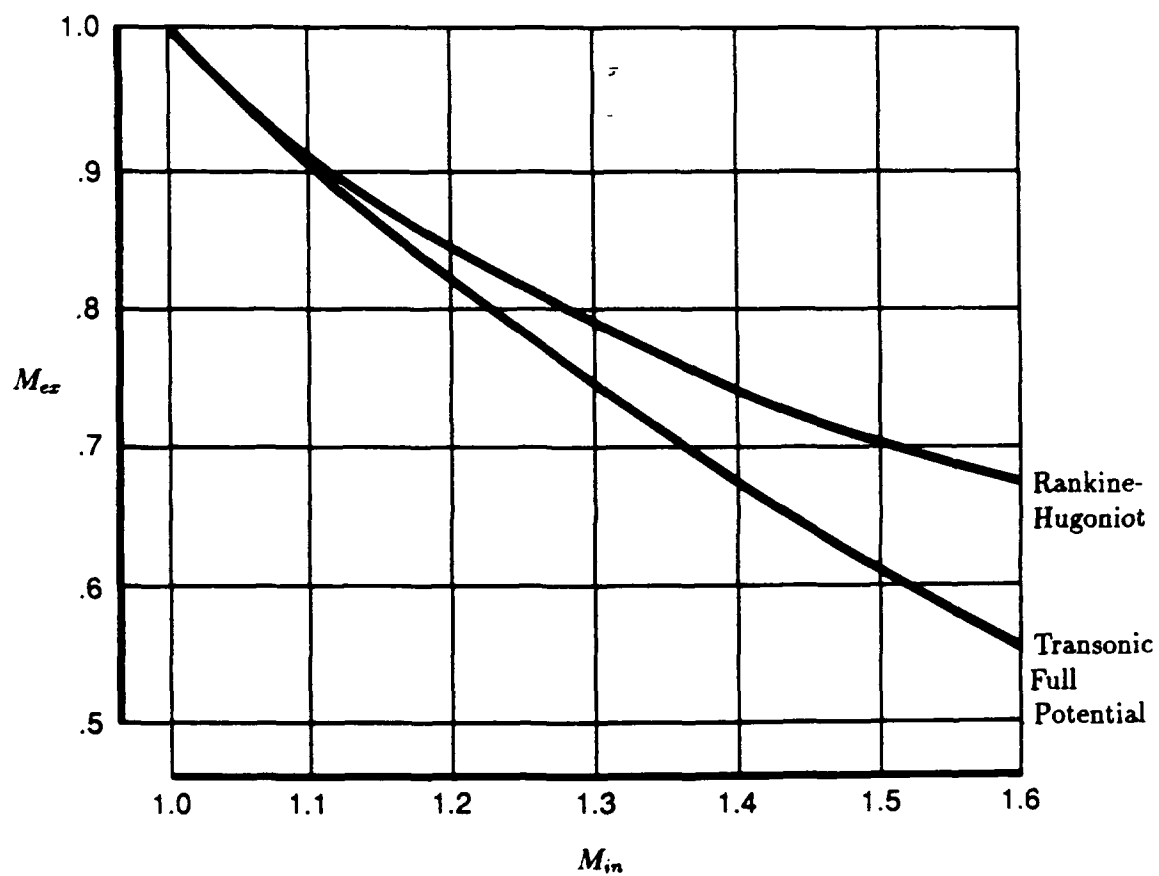
18

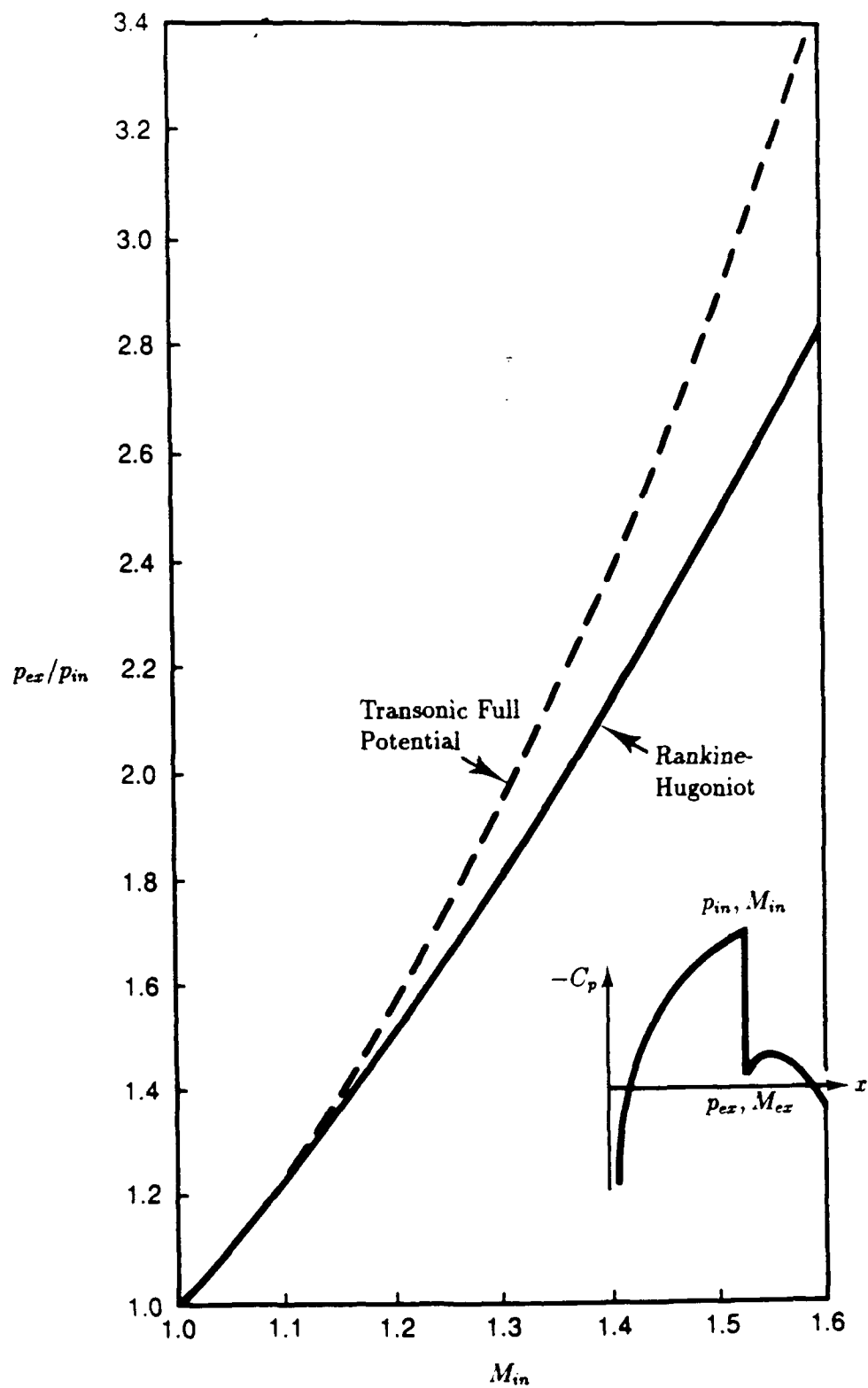Fig 2.   Exit Mach Numbers for Normal Shocks
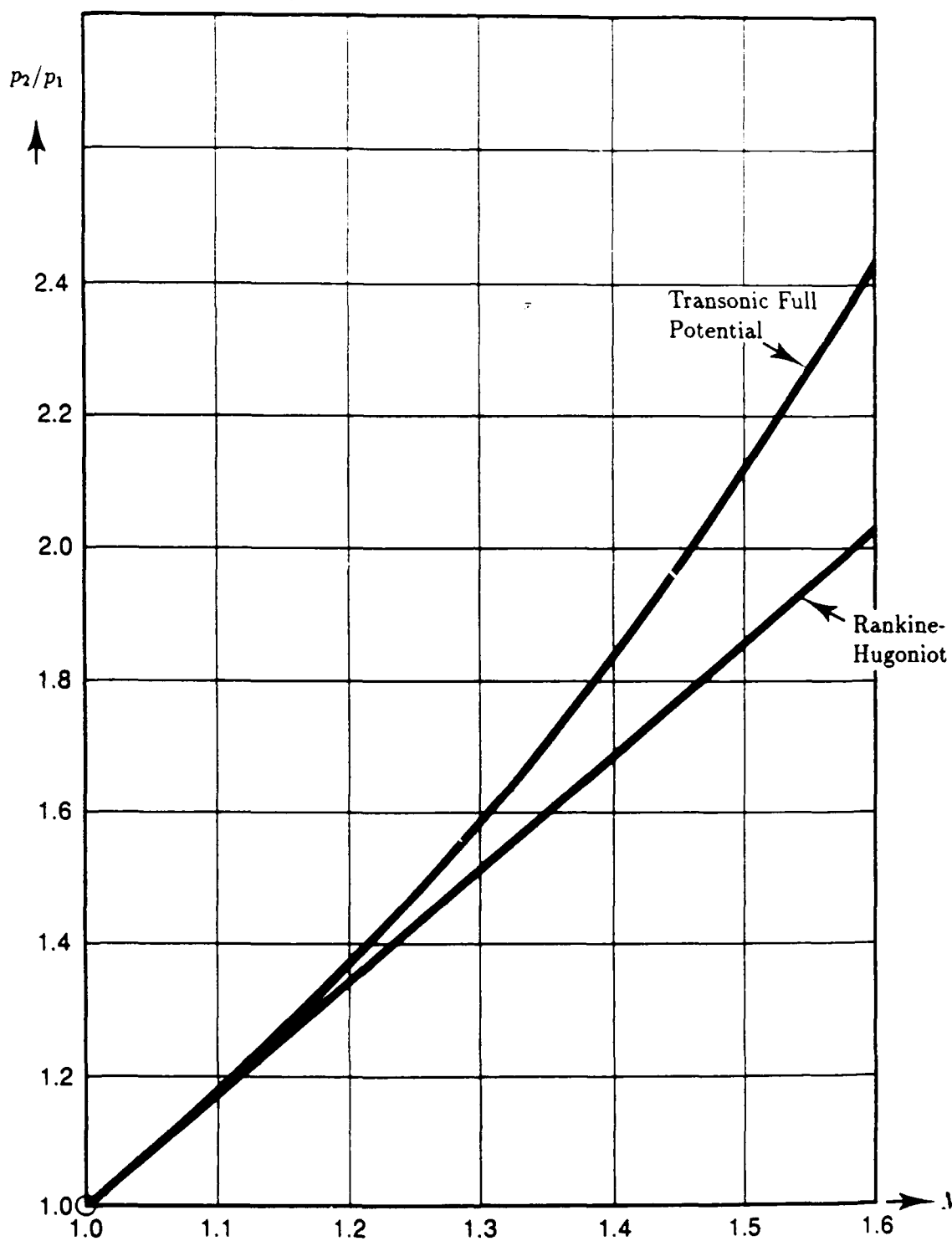
Fig 3. Pressure Ratios for Normal Shocks

Fig 4.   Density Ratios for Normal Shocks

$\dot{\rho} = \rho/\rho_\infty^*$

1.8

SUPERSONIC

SUBSONIC

1.6

Full Potential Equation
Shock Exit

$\hat{\rho} = \hat{\rho}_{is}$

C

1.4

1.2

II

True Shock
Exit

B

(1, 1)

1.0

$\rho = \left(\frac{\gamma+1}{2} - \frac{\gamma-1}{2}\hat{q}^2\right)^{\frac{1}{(\gamma-1)}} (= \hat{\rho}_{is})$
(Equation (7))

Equation (4')

.8

$\hat{\rho} = \left\{\left(\frac{\gamma+1}{2}\hat{q}^2 - \frac{\gamma-1}{2}\right)^{\frac{1}{(\gamma-1)}}\right\} / \hat{q}^{\frac{2\gamma}{(\gamma-1)}} (= \hat{\rho}_{ex})$
(Equation (9))

Shock
Entry

.6

A

$(\hat{q}_1, \hat{p}_1)$

$\hat{\rho}\hat{q} = \hat{\rho}_1\hat{q}_1$
(Equation (1'))

.4

.2

$\hat{q} = q/q_\infty^*$

0

0.5   1.0   1.5   2.0   2.5   3.0

$1/\sqrt{6} = 0.408_{25}$
$(M_{ex} = 1/\sqrt{7})$
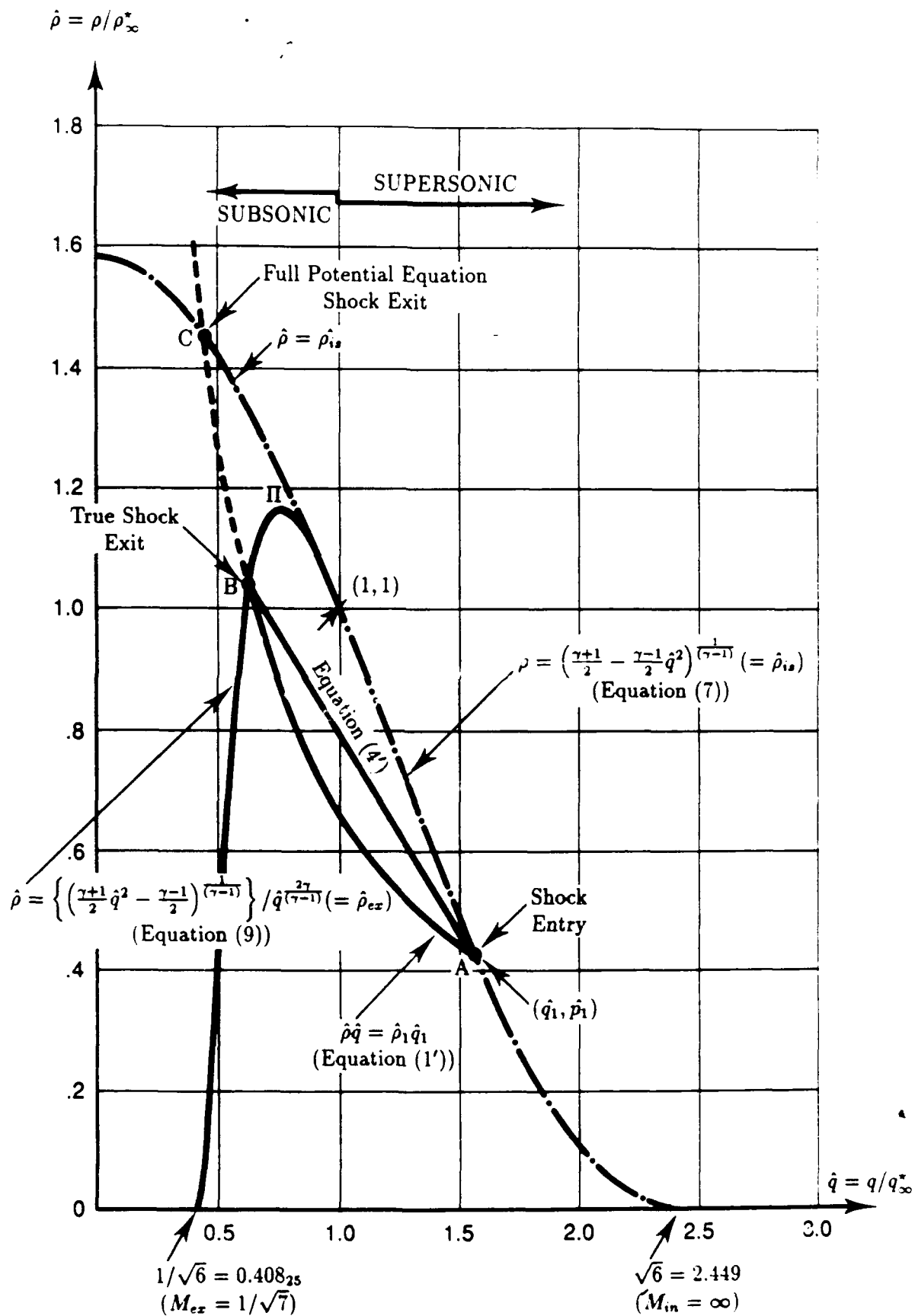
$\sqrt{6} = 2.449$
$(M_{in} = \infty)$

Fig 5.   ($\hat{\rho}$ vs $\hat{q}$) Relationships for Isentropic Flow and for Normal Shock Waves
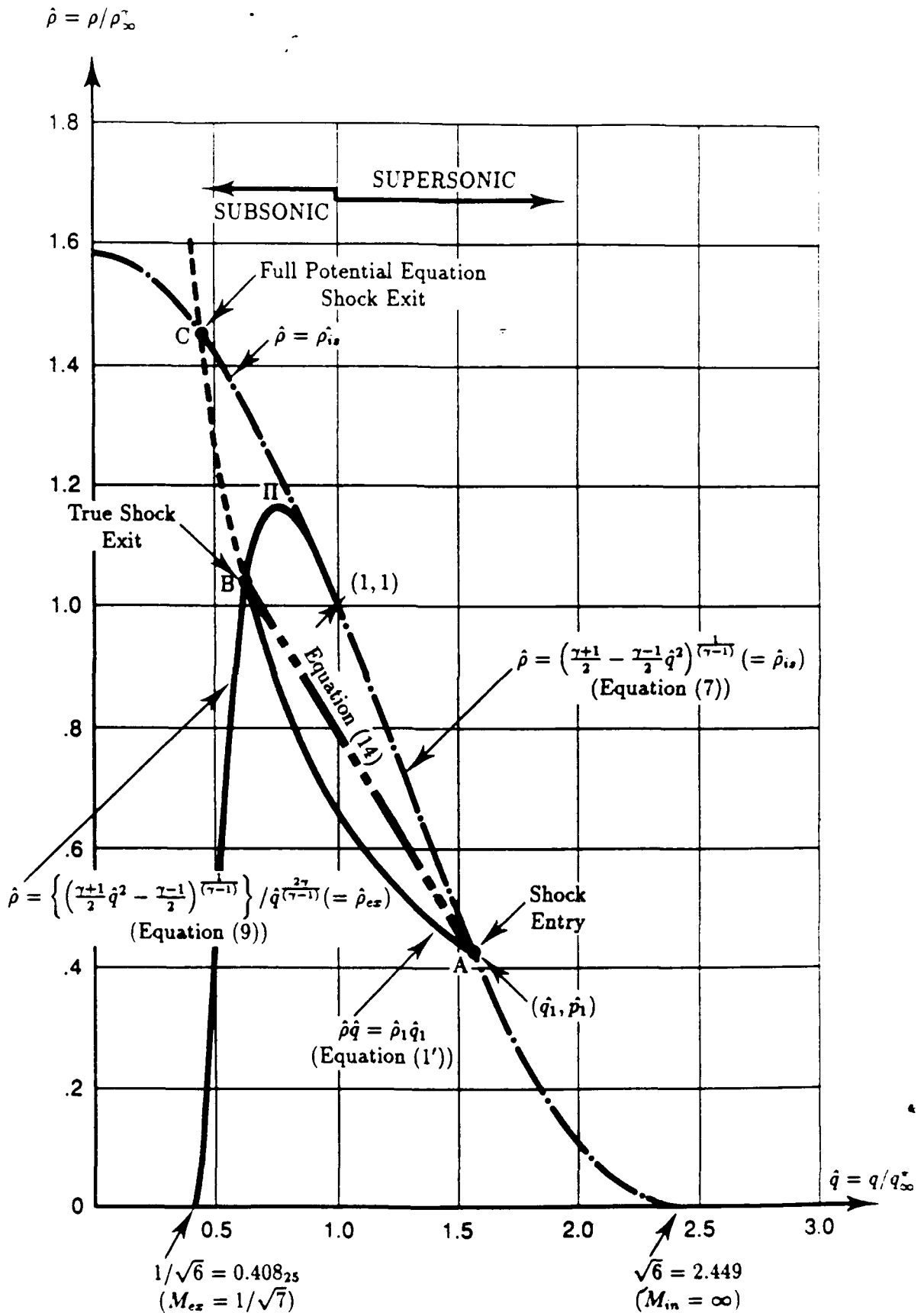
Fig 6. ($\hat{\rho}$ vs $\hat{q}$) Relationships for Isentropic Flow and for Normal Shock Waves (with Equation 14)

DISTRIBUTION

AUSTRALIA

Department of Defence

Defence Central
Chief Defence Scientist)
AS, Science Corporate Management) shared copy
FAS Science Policy)
Director, Departmental Publications
Counsellor, Defence Science, London (Doc Data sheet only)
Counsellor, Defence Science, Washington (Doc Data sheet only)
Scientific Adviser, Defence Central
OIC TRS, Defence Central Library
Document Exchange Centre, DSTIC (8 copies)
Defence Intelligence Organisation
Librarian H Block, Victoria Barracks, Melbourne (Doc Data sheet only)

Aeronautical Research Laboratory
Director
Library
Chief Flight Mechanics and Propulsion
Branch Head - Flight Mechanics
Branch File - Flight Mechanics
Author: B.W.B Shaw
B.D. Fairlie

Navy Office
Navy Scientific Adviser (3 copies Doc Data sheet only)

Army Office
Scientific Adviser - Army (Doc Data sheet only)

Air Force Office
Air Force Scientific Adviser (Doc Data sheet only)

SPARES (4 COPIES)

TOTAL (24 COPIES)

DOCUMENT CONTROL DATA

PAGE CLASSIFICATION
UNCLASSIFIED

PRIVACY MARKING

1a. AR NUMBER AR-006-105	1b. ESTABLISHMENT NUMBER ARL-FLIGHT-MECH TM-424	2. DOCUMENT DATE OCTOBER 1991	3 TASK NUMBER DST 91/40

4. TITLE
A RANKINE-HUGONIOT EMULATING (DENSITY vs. VELOCITY) RELATIONSHIP FOR CFD USAGE WITHIN AN INVISCID SHOCK WAVE

5. SECURITY CLASSIFICATION
(PLACE APPROPRIATE CLASSIFICATION IN BOX(S) IE. SECRET (S), CONF. (C) RESTRICTED (R), UNCLASSIFIED (U)).

U	U	U
DOCUMENT	TITLE	ABSTRACT

6. NO. PAGES
26

7. NO. REFS.
15

8. AUTHOR(S)
B.W.B. SHAW

9. DOWNGRADING/DELIMITING INSTRUCTIONS
Not applicable

10. CORPORATE AUTHOR AND ADDRESS

AERONAUTICAL RESEARCH LABORATORY

506 LORIMER STREET

FISHERMENS BEND VIC 3207

11. OFFICE/POSITION RESPONSIBLE FOR:

SPONSOR _____ DSTO _____

SECURITY _____ - _____

DOWNGRADING _____ - _____

APPROVAL _____ CFPD _____

12. SECONDARY DISTRIBUTION (OF THIS DOCUMENT)

Approved for public release

OVERSEAS ENQUIRIES OUTSIDE STATED LIMITATIONS SHOULD BE REFERRED THROUGH DSTIC, ADMINISTRATIVE SERVICES BRANCH, DEPARTMENT OF DEFENCE, ANZAC PARK WEST OFFICES, ACT 2601

13a. THIS DOCUMENT MAY BE ANNOUNCED IN CATALOGUES AND AWARENESS SERVICES AVAILABLE TO . . . .

No limitations

13b. CITATION FOR OTHER PURPOSES (IE. CASUAL ANNOUNCEMENT) MAY BE

[X] UNRESTRICTED OR [ ] AS FOR 13a.

14. DESCRIPTORS

Transonic flow　　　　Zonal solutions
Inviscid flow　　　　Full potential equation
Shock waves
Computational fluid dynamics
Rankine-Hugoniot equations

15. DISCAT SUBJECT CATEGORIES

2004

16. ABSTRACT
To enable the Full Potential Equation method of computing transonic inviscid flows to accurately predict the conditions at exit from a shock wave - a desirable aim which the method fails to achieve to a greater or lesser extent - an improved relationship has been derived between the density (p) and velocity (q) inside an inviscid shock wave. This relationship replaces the conventional isentropic, isenergic relationship normally applied there. The shock exit conditions thereby obtained are the correct Rankine-Hugoniot values, for all shock inlet Mach numbers.

Zonal application of this improved (p,q) shock wave internal relationship should eliminate the prime cause of solution inaccuracy when using the conservative Full Potential Equation method.